PHYSICAL REVIEW A **68**, 052707 (2003)

Determination of the β parameter for atomic Mn and Cr $2p$ photoemission: A benchmark test for core-electron photoionization theories

Kai Godehusen and Philippe Wernet
BESSY GmbH, Albert-Einstein-Straße 15, D-12489 Berlin, Germany

Tobias Richter and Peter Zimmermann
Technische Universität Berlin, Hardenbergstraße 36, D-10623 Berlin, Germany

Michael Martins
Universität Hamburg, Luruper Chaussee 149, D-22761 Hamburg, Germany

(Received 6 August 2003; published 6 November 2003)

We have determined the anisotropy parameter β for the electron angular distribution in direct $2p$ photoionization of free Mn and Cr atoms. By using a high-resolution electron spectrometer and by rotating the polarization axis of the linearly polarized synchrotron radiation the values for β could be derived with high precision and separately for the different multiplet components. Combination of the experimental results with Hartree-Fock based single configuration and multiconfiguration *ab initio* calculations gives new insight into the atomic $3d$-metal $2p$ photoionization process. Configuration interaction in the final ionic states need to be taken into account to adequately describe the measured photoelectron angular distributions.

DOI: 10.1103/PhysRevA.68.052707 PACS number(s): 32.80.Fb, 32.80.Hd

I. INTRODUCTION

In the past few years substantial improvements have been made in the theoretical calculation of photoemission spectra of $3d$ transition metals, both in the gas phase and the solid phase, and also for transition-metal compounds (see Refs. [1–10] and references therein).

This has led to new insights into the electronic structure of these technologically relevant elements. In this context, the analysis of electron spectroscopy data from free $3d$-metal atoms with the aid of *ab initio* calculations also leads to valuable information on condensed-matter systems (see, e.g., Refs. [1,2]).

In the past the $3p$ and $2p$ photoelectron spectra of free Cr and Mn atoms have been successfully analyzed both in terms of multiplet splittings and relative cross sections. For laser-polarized Cr atoms the dichroism in $3p$ and $2p$ photoemission gave additional insight into the dynamics of the photoionization process [2–5,11]. Linear alignment dichroism (LAD) as measured with aligned atoms and linear magnetic dichroism in the angular distribution (LMDAD) for oriented atoms both measured with linearly polarized ionizing radiation [2,3,11] give access to the phases of the outgoing free-electron waves and thus in principle allow for complete experiments [12].

Corresponding dichroism measurements on laser-polarized Mn atoms are hampered to date due to missing efficient optical pumping schemes. We therefore chose to investigate the dynamics of the Mn $2p$ photoionization process using a different approach, namely, by studying the anisotropy parameter β in the $2p$ photoelectron angular distribution. This is done here by rotating the polarization axis of the ionizing synchrotron radiation which represents a new and highly accurate way to measure the angular distribution of photoelectrons [13]. This method enabled us to measure the core-level photoelectron angular distribution of free metal vapors. Only very sparse experimental data on the direct measurement of β for atomic $3d$ transition metals exist yet. So far only the $3p \rightarrow 3d$ resonance region for atomic Mn [14,15] and Sc [16] have been investigated.

Results for measured and calculated β parameters for the $2p$ photoemission of free Mn and Cr atoms and separately for different multiplet components are presented. High-resolution photoelectron spectra are combined with the additional information about β and pose a surprisingly strong test to the results of *ab initio* calculations. With the new data presented here, we can demonstrate that the single configuration approximation, which was thought to be sufficient for the description of the spectra, has to be expanded. A more complex multiconfiguration calculation has to be applied.

In the following, we will first introduce the experimental setup and calculation methods used, then we will present β independent photoelectron spectra and discuss the $2p$ multiplet structure of Mn and Cr. In the main part of this paper we will discuss the angle-resolved measurements together with the results of the calculations, including calculated Mn $2p$ dichroism spectra. In the Appendix we analytically derive a formula for β in the case of a pure jj or jK coupling scheme.

II. THEORY AND EXPERIMENT

For the photoionization of an unpolarized (unoriented) target by linearly polarized radiation and within the dipole approximation, the differential cross section is defined by Yang's [17] theorem:

$$\frac{d\sigma}{d\Omega}(\theta)=\frac{\sigma}{4\pi}[1+\beta P_2(\cos\theta)]. \tag{1}$$

Here θ is the angle between the polarization vector of the ionizing light and the momentum vector of the ejected electron, $P_2(x)=\frac{1}{2}(3x^2-1)$ is the second Legendre polynomial, and σ is the angle independent cross section of the investigated ionization process. Detection of the photoelectrons at angle θ of 54.7° (the so-called magic angle) relative to the polarization axis of the ionizing radiation results in a spectrum directly proportional to σ, since $P_2[\cos(54.7°)]=0$. This is the β independent spectrum.

Determination of the anisotropy parameter β is of great interest since β offers additional information on the photoionization process. In contrast to the cross section it also depends on the sign of the matrix elements and the phases of the outgoing (free-) electron waves. The experimental determination of β is therefore supplementary to that of the relative cross section of the multiplets.

To measure the angular distribution of the photoelectrons we used the ability of the BESSY II UE52-SGM beam line to rotate the polarization axis of the linearly polarized undulator radiation. With this method the angle accuracy is better than 0.2° and the degree of linear polarization is above 96% for any orientation of the polarization plane (see Ref. [13]). The photoelectrons have been recorded using a high-resolution Scienta SES-2002 electron analyzer. Only electrons emitted perpendicular to the propagation direction of the synchrotron radiation have been detected. Possible quadrupole effects in the angular distribution are thus eliminated [18–20].

A detailed description of the experimental setup and the advantages of this high-precision method have been published recently [13].

Theoretical spectra were calculated both in single configuration approximation using the Hartree-Fock (HF) approximation and in multiconfiguration approach using the configuration interaction (CI) method to study the influence of correlations on the photoelectron spectra. To take into account the weak configuration interaction with the large number of high-lying configurations, all Slater integrals were scaled by 85% of their *ab initio* values [11]. Note that for the Mn and Cr $3p$ photoemission in Ref. [11] a scaling of 80% has been used, in the case of $2p$ photoemission the multiplet splitting is better reproduced by a scaling of 85%. For the spin-orbit parameters, the *ab initio* values have been used. Matrix elements were calculated in an intermediate coupling scheme with the standard Slater-Condon superposition of configuration method using the COWAN Code [21] including relativistic corrections.

To derive the values of β from the HF and CI calculations the following formalism was applied (see Ref. [3] for more details). The β parameter can be expressed in terms of the generalized anisotropy parameters $\beta_{k_0kk_\gamma}$, which describe the dynamics of the photoionization process. The k_0kk_γ represent the rank of the statistical tensors describing the initial atomic state (k_0), the combined state of ion+photoelectron (k), and the state of the ionizing photons (k_γ). For detail on the theory of atomic angular distributions see Ref. [22]. The β parameter is determined by

$$\beta=-\sqrt{\frac{10}{3}}\beta_{022} \tag{2}$$

with

$$\beta_{022}=\frac{B_{022}}{\sum\limits_{Jlj}|\langle\alpha_fJ_f,\varepsilon lj:J||D||\alpha_0J_0\rangle|^2}. \tag{3}$$

The coefficient B_{022} is given by [22]

$$\begin{aligned}B_{022}=3\hat{J}_0\sum_{JJ'll'jj'}&(-1)^{J+J_f+3/2}\hat{J}\hat{J}'\hat{j}\hat{j}'\hat{l}\hat{l}'(l0,l'0|20)\\&\times\begin{Bmatrix} j & l & \frac{1}{2}\\ l' & j' & 2\end{Bmatrix}\begin{Bmatrix} j & l & J_f\\ J' & j' & 2\end{Bmatrix}\begin{Bmatrix} J_0 & 1 & J\\ J_0 & 1 & J'\\ 0 & 2 & 2\end{Bmatrix}\\&\times\langle\alpha_fJ_f,\varepsilon lj:J||D||\alpha_0J_0\rangle\\&\times\langle\alpha_fJ_f,\varepsilon l'j':J'||D||\alpha_0J_0\rangle^*.\end{aligned} \tag{4}$$

Here, J_0, α_0 (J_f,α_f) characterize the initial (final) state of the atom (ion), l, j are the orbital and angular momenta of the photoelectron, and $\langle\alpha_fJ_f,\varepsilon lj:J||D||\alpha_0J_0\rangle$ are the multichannel dipole amplitudes. The standard notations for the Clebsch-Gordan coefficients and the Wigner nj coefficients are used and $\hat{J}=\sqrt{2J+1}$.

With these formulas the β parameter can be calculated by inserting the HF or CI dipole matrix elements $\langle\alpha_fJ_f,\varepsilon lj:J||D||\alpha_0J_0\rangle$ in Eq. (4).

In the Appendix of this paper we present the analytical calculation of β which is possible with the assumption of a pure coupling scheme.

III. β INDEPENDENT PHOTOELECTRON SPECTRA

Figure 1 shows the β independent photoelectron spectra of Mn and Cr measured at the magic angle and taken at a photon energy of 850 eV and 720 eV, respectively. The spectra are proportional to the cross section and do not contain any influence of the angular distribution. Compared to previously published spectra we have been able to improve resolution and statistics considerably by measuring at the third generation synchrotron source BESSY II in Berlin, Germany.

Figure 1 also shows the results of our *ab inito* HF calculations including only one valence electron configuration: $3d^54s^2$ for Mn ($3d^54s$ for Cr) for both the initial and the final ionic states. The calculated spectra have been convoluted with Gaussian profiles with 0.8 eV full width at half maximum for Mn and 0.7 eV for Cr to account for the lifetime broadening and for the experimental resolution, which was determined by rare-gas measurements to be 0.5 eV. Additionally the spectra had to be shifted by 1.8 eV (Mn) and 0.8 eV (Cr) towards lower binding energies to match with the experimental ones (this holds for all the spectra shown in this paper).

As one can easily see there is excellent agreement between the experimental spectra and the calculated ones. Since the structure of the β independent $2p$ spectra of Mn and Cr has been discussed before (see Refs. [3,4]), we want

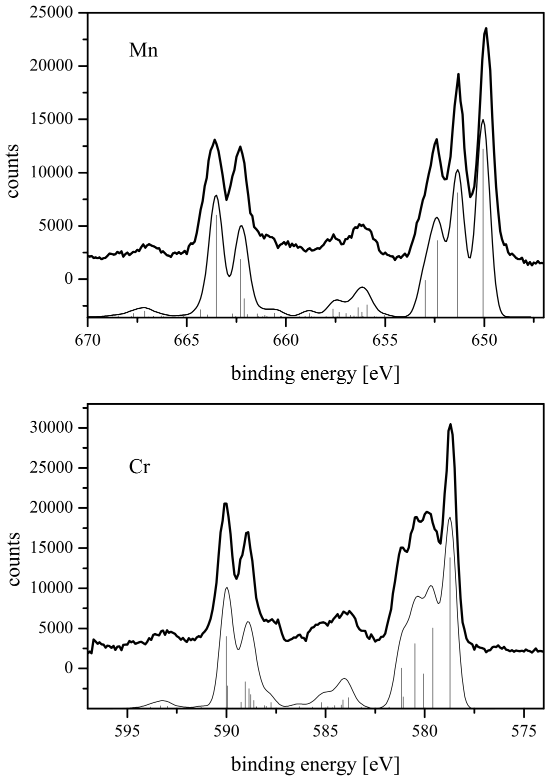

FIG. 1. $2p$ photoelectron spectra of Mn and Cr taken at photon energies of 850 eV and 720 eV, respectively The results of the single configuration HF calculations (thin line) are convoluted with Gaussian profiles of 0.8 eV and 0.7 eV width, respectively.

to concentrate here on the main features.

The spectra are each dominated by two groups of lines. The energy separation of these groups is due to the spin-orbit splitting of the $2p$ core hole. The Coulomb interactions of the $2p$ hole and the $3d$ valence electrons cause the final-state splitting reflected in the multiplet features spread over several eV, instead of a single "$2p_{1/2}$" and a single "$2p_{3/2}$" line. A first approach using a pure coupling scheme (namely, jK coupling) yields four components in the $2p_{3/2}$ multiplet with angular momenta $J_f=4$, 3, 2, and 1 for Mn ($J_f=9/2$, 7/2, 5/2, and 3/2 for Cr) and two components in the $2p_{1/2}$ multiplets with $J_f=3$ and 2 for Mn ($J_f=7/2$ and 5/2 for Cr). The approximations for this approach are briefly summarized in the Appendix. Recoupling of the $3d$ valence electrons leads to additional important features: it gives rise to satellite lines and changes character and intensities of the main lines. This recoupling can be viewed as the spin flip of one or two of the $3d$ valence electrons. The main lines may now be described as a mixture of Hund's rule ground-state $3d^5\,{}^6S$ and spin-flip $3d^5\,{}^4L$, ${}^2L$ states (the $4s$ electrons are omitted for clarity). The two spin-orbit split groups of satellites with mainly spin-flip $3d^5\,{}^4L$ character lie between the multiplets and on the high binding energy side of the spectra. The double-spin-flip $3d^5\,{}^2L$ states overlap with the $2p_{1/2}$ multiplet and are located at the high binding energies outside the range shown in Fig. 1. Recoupling of the $4s$ shell in Cr complicates the situation and gives rise to the characteristic shape of the $2p_{3/2}$ multiplet with less fine structure compared to Mn due to additional lines (see HF calculation in Fig. 1). Tables I and III summarize the assignments of the strongest lines according to the single configuration HF calculation. More information can be found in Refs. [3,4].

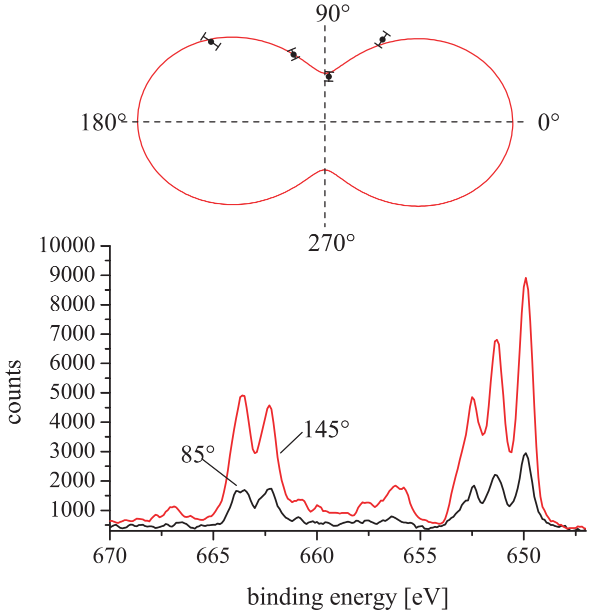

FIG. 2. Bottom: $2p$ photoelectron spectrum of Mn at 850 eV photon energy, measured for the angles 85° and 145°. Top: polar plot of the intensity of the strongest Mn photoemission line (at 650.06 eV binding energy), for four different angles.

Tables I and III show that nearly all lines consist of a mixture of the different couplings of the $3d$ electrons. From Table III it can be seen that the coupling for Cr is more complex than that for Mn, because of the open $4s$ shell [3]. The single configuration approximation yields 214 lines for Mn and 417 for Cr, which demonstrates the complexity of the couplings involved even for this approximation.

IV. ANGULAR DISTRIBUTION MEASUREMENTS

A. Manganese

The key element of the method used to measure the angular distribution is to rotate the polarization axis of the linearly polarized ionizing light with high accuracy whilst keeping the detector position fixed in space.

The bottom part of Fig. 2 shows the Mn $2p$ photoemission spectra taken for two different angles between spectrometer and polarization axis. One can see the variation of intensity as a function of the angle. This variation is quite uniform for the whole spectrum. $2p$ photoemission spectra for Mn and Cr were taken for four different angles each. The upper part of Fig. 2 shows the intensity of the strongest Mn line (at 650.06-eV binding energy) at these four angles together with a fitted angular distribution curve [Eq. (1)].

For each angle the spectra were fitted with an appropriate number of Voigt profiles. Four (five) profiles were assumed to mainly contribute to the $2p_{3/2}$ multiplet of Mn (Cr), two profiles to the satellites, and two to the $2p_{1/2}$ multiplet. Only

TABLE I. Results of the single configuration HF calculation for Mn at a photon energy of 850 eV. Note that due to the small splitting of some of the calculated lines in this table, not all of them could be resolved in the experimental spectra (especially in the satellites), therefore only the experimental values for β for the stronger lines are given. This holds for all the tables in this paper. The total angular momentum of the ion J_f, the total angular momentum of the $2p$ core-hole j, and the contribution of the strongest LS coupling term of the $3d$ valence electrons (in %) according to the HF calculations are given for assignment.

Experiment			HF calculation			Assignment			
Energy (eV)	Intensity	β	Energy (eV)	Intensity	β	J_f	j	$3d^5$	%
649.90	100	1.05 ± 0.09	650.06	100.0	1.31	4	3/2	^6S	100
651.32	80	1.00 ± 0.12	651.34	74.0	1.07	3	3/2	^6S	91
652.34	46	1.00 ± 0.09	652.32	45.5	1.24	2	3/2	^6S	77
653.09	18	1.00 ± 0.09	652.98	21.9	1.31	1	3/2	^6S	64
656.20	35	1.01 ± 0.17	655–657.2	23.2	1.17		3/2	^4L	
657.7	9	1.01 ± 0.17	657.2–658.7	9.3	1.31		3/2	^4L	
			662.11	10.9	1.24	2	3/2	^2G	28
662.31	59	1.13 ± 0.12	662.29	34.4	1.22	2	1/2	^6S	55
663.65	70	1.19 ± 0.10	663.52	60.7	1.28	3	1/2	^6S	71
			664.30	4.4	1.29	3	3/2	^2P	71

the area of the profiles was varied between the fits for different angles, the positions and widths were kept constant. In this way the intensity variation of each line under rotation of the polarization direction was determined. These experimental values were fitted with the angular distribution [Eq. (1)] with σ and β as free parameters. Thus multiplet resolved values for β could be derived, as shown in Tables I–IV, and are compared with the ones derived from our HF calculations.

The results of the HF calculation for Mn considering only a single $3d^5 4s^2$ configuration are listed in Table I together with the experimental values for β. The experimental values are, within the error bars, constant over the whole multiplet; a fact that could already be seen from Fig. 2 where no significant changes in relative intensities of different multiplet components could be observed. The calculated values differ from experiment in two respects: they are larger than the experimental ones and they are significantly different for different multiplet components. The former discrepancy can be explained by a deviation between the calculated and real phase shift between the outgoing waves. The calculation delivers a single value of this shift for all lines of the multiplet, therefore a deviation will lead to a general mismatch for all lines of the multiplet. Such a deviation of the phase shift can easily be explained by imperfect modeling of the potential seen by the $2p$ electrons within the calculations.

Far more important is the fact that the calculated values are not constant over the multiplet in contrast to the measured ones. We will now look into this in more detail.

To have a better visual comparison between experiment and calculation Fig. 3 shows the spectra of the $2p_{3/2}$ multiplet measured under an angle of 85° and 145° (left panel). The spectra are scaled so that the strongest lines $(J=4)$ match in intensity. This way the deviation from a uniform β value for these lines should be easily discernible (i.e., since the curves are nearly identical, the value of β for all lines is almost the same). Doing the same for the single configuration HF calculations [middle panel, using the calculated cross sections and β values inserted in Eq. (1)] results in two curves that show a significant deviation in the second strongest line (accordingly see the calculated β parameter for line at 651.34 eV in Table I).

To further investigate the reason for this discrepancy, we expanded our single configuration HF calculations and additionally included the valence configurations $3d^6\ 4s$ and $3d^7$ for the ionic states. The result can be seen in the right panel of Fig. 3. It is a big improvement over the single configuration calculation. In Table II the results of the multiconfiguration calculation for Mn are listed. The calculated values for β are now quite uniform across the multiplet, like the experimental ones. Still the calculated values are slightly larger than the experimental results. Among the strongest lines two new lines appear at 652.34 eV and 663.64 eV binding energy which have a main contribution of $3d^7$ and $3d^6$, respectively. Though only very few lines in Table II are affected by

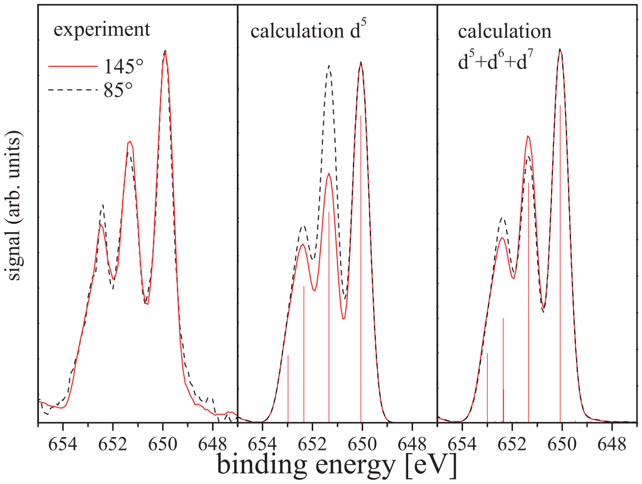

FIG. 3. Comparison of the single and the multiconfiguration calculations with the experimental results for Mn. The spectra of the $2p_{3/2}$ multiplet measured under the angles of 85° and 145° are scaled to the most intense line, the same is done with the calculated results (see text), the bar graphs shown correspond to an angle of 145°.

TABLE II. Results of the multiconfiguration CI calculation (including $3d^5$, $3d^6$, and $3d^7$) for Mn at a photon energy of 850 eV.

	HF calculation		Experimental		Assignment		
Energy (eV)	Intensity	β	β	J_f	$3d^5$	$3d^6$	$3d^7$
650.08	100.0	1.25	1.05±0.09	4	⩾98%		
651.34	74.4	1.30	1.00±0.12	3	⩾98%		
652.34	10.6	1.19	1.00±0.09	2	27%	17%	56%
652.36	33.9	1.16	1.00±0.09	2	86%	4%	10%
653.00	21.6	1.30	1.00±0.09	1	98%	2%	
656-657.2	23.5	1.05	1.01±0.17		99%	1%	
657.2-658.7	10.0	1.30	1.01±0.17		⩾98%		
662.12	11.7	1.00		2	98%	2%	
662.30	33.3	1.24	1.13±0.12	2	97%	3%	
663.51	53.1	1.21	1.19±0.10	3	91%	9%	
663.64	6.7	1.27		3	10%	90%	
664.32	3.4	1.20		3	84%	16%	

an admixture of additional configurations by more than a few percent, the β parameter changes for all of them. Note in particular the improvement for the second main line at 651.34 eV (Table II and Fig. 3). This shows that the interaction with the $3d^6$ and $3d^7$ configurations is essential for the description of the photoionization process.

In the Appendix of this paper we calculate analytically the formula for β for the simplified case of a pure coupling scheme, a single configuration, and a frozen valence shell. The result [Eq. (A4)] is independent of the final ionic state (i.e., independent of J_f) and thus β is the same for all lines of the multiplet within the approximations. It is obvious that the assumption of a pure coupling scheme is not valid for the description of the $2p$ photoionization of atomic Mn and Cr. Nevertheless upon first sight the uniformity of the experimental β values seem to comply with the analytical formula. But the assumption of a pure coupling scheme can only serve as a zero-order approximation of the actual $2p$ photoionization, since it fails to describe many features, regarding the multiplet structure and the dichroism, seen in the experiment. For the necessary intermediate coupling scheme the analytical formulation of β is not possible and Eq. (4) has to be solved numerically.

From our HF and CI calculations we can not only derive the β independent cross section and β but also LAD and LMDAD spectra. Like β the LAD and LMDAD depend on the generalized anisotropy parameters $\beta_{k_0 k k_\gamma}$. Neglecting higher-order effects the LMDAD is determined by β_{122}, whereas the LAD is determined by β_{220}, β_{202}, β_{222}, and β_{242}. This is described in detail in Refs. [2,3].

We now want to compare the β independent cross section and the dichroism for the two calculations (HF and CI). Figure 4 shows that the calculated β independent Mn $2p$ photoelectron spectrum does not change noticeably going from the single configuration to the multiconfiguration calculations. Though the number of resulting states increases from 214 to 684, the convoluted spectrum still looks the same. This is an important finding, since it demonstrates that on the basis of the cross section alone the quality of the HF calculation results cannot be judged. Even the dichroism (LAD and LMDAD) is not sensitive enough to do this as the following discussion will show. In contrast to Cr, there are no experimental investigations on the dichroism of free, polarized Mn atoms available yet.

The dichroism of the single configuration and the multi configuration calculations are both shown. Though individual calculated lines show a change in the order of that seen in β between the two calculations, the effect in the

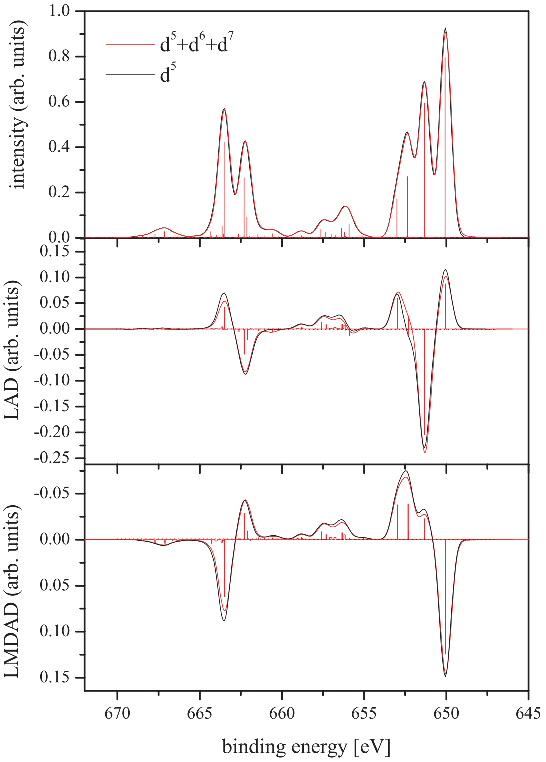

FIG. 4. Calculated β independent cross section, LAD, and LMDAD spectra for Mn at 850 eV photon energy. Shown are the results both from the single configuration and the multiconfiguration calculation. For the multiconfiguration calculation results a bar graph is shown. For the cross section (top panel) the two curves are indistinguishable.

TABLE III. Results of the single configuration HF calculation for Cr at a photon energy of 720 eV. For the description see caption of Table I.

Experiment			HF calculation				Assignment			
Energy (eV)	Intensity	β	Energy (eV)	Intensity	β	J_f	j	$3d^5$	$3d^5 4s$	%
578.71	100	1.04±0.10	578.72	100.0	1.23	9/2	3/2	^6S	^7S	100
579.66	55	1.09±0.10	579.59	53.5	1.09	7/2	3/2	^6S	^7S	66
580.15	23	1.09±0.10	580.08	23.2	1.13	7/2	3/2	^6S	^5S	67
580.55	44	1.08±0.10	580.50	43.2	0.79	5/2	3/2	^6S	^7S	69
			581.09	7.9	1.21	5/2	3/2	^6S	^5S	72
581.27	42	1.02±0.10	581.18	27.0	1.25	3/2	3/2	^6S	^7S	67
583.85	32	1.05±0.12	582.8–584.8	22.4	1.20		3/2	^4L		
585.35	21	1.05±0.12	584.8–586.5	11.5	1.24		3/2	^4L		
587.86	27	1.05±0.10	587.76	4.2	1.16	5/2	3/2	^2S		25
588.92	42	1.05±0.10	588.62–588.86	28.3	1.13	5/2	3/2	^2L		
			589.06	17.9	1.11	5/2	1/2	^6S	^7S	26
			589.26	4.4	1.17	7/2	3/2	^2F		19
			589.94	15.16	1.21	7/2	3/2	^2G		25
590.00	88	1.05±0.10	590.01	47.9	1.19	7/2	1/2	^6S	^7S	55

convoluted spectra is only very small. This is due to the nature of the dichroism where the sign changes hide the changes in the intensity of a single line. The resulting difference in the dichroism for the two calculations is too small to be discerned by present experiments. That means that on the basis of the cross section and the dichroism both calculations yield spectra that are almost indistinguishable.

It is interesting to note that the calculated LAD in Mn $2p$ photoionization shows a large intensity for the $2p_{1/2}$ multiplet (Fig. 4) comparable to the case for Cr $2p$ [3]. This is a direct consequence of the mixing of $2p_{1/2}$ and $2p_{3/2}$ core-hole states in the high binding-energy multiplet due to the near degeneracy of Hunds' rule ground-state $2p_{1/2}\ 3d^5\ ^6S$ and double-spin-flip $2p_{3/2}\ 3d^5\ ^2L$ levels in the corresponding binding-energy region [3].

As it turns out, the β parameter is not simply an additional tool to test state-of-the-art *ab initio* calculations but a very powerful one, showing deviations that cannot be seen otherwise.

B. Chromium

Now looking at Cr we will see that the situation is similar. Figure 1 displays the β independent Cr $2p$ photoemission spectrum together with the results of a single configuration calculation including only states with $3d^5$.

In the same manner as for Mn, also for Cr the β parameter has been determined. These results are shown together with the results of the single configuration calculation in Table III.

The results resemble very much that for Mn, the measured values for β are uniform across the whole spectrum, whereas the calculated ones are not as uniform and also generally slightly too large. To our belief, the overestimation of β by the calculation in this case can also be attributed to an approximation in the calculation method used. The generally accepted way to account for the weak configuration interaction with the large number of high-lying configurations is to scale the Slater integrals to 85% of their *ab inito* values, this yields good results for the dipole matrix elements. As mentioned above, the phase difference is very sensitive to the atomic potential and therefore to an incomplete modeling of it. To investigate this, we performed a CI calculation for Mn were the Slater integrals have been scaled to 90%. It resulted, as expected, in a slightly larger multiplet splitting which does not match as well as the experimental data. But the remarkable finding is that the different scaling does not change the derived values for β. This means that the scaling has only a very small effect on β and that the only way to model the atomic potential more accurately in terms of the angular distribution is to include the high-lying configurations, which is yet impossible due to the large number of configurations that would have to be considered.

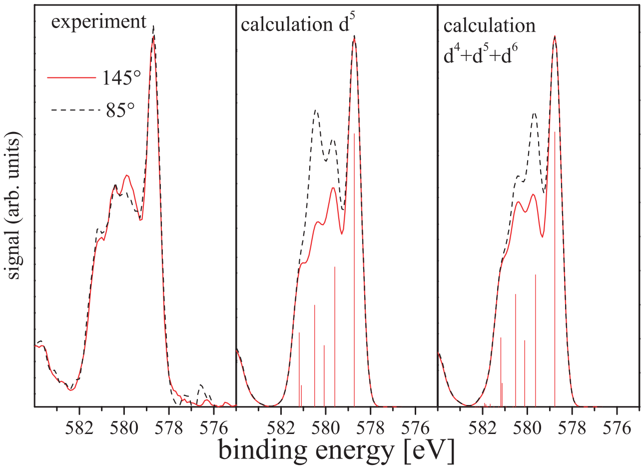

FIG. 5. Comparison of the single configuration and the multiconfiguration calculations with the experimental results for Cr. The spectra of the $2p_{3/2}$ multiplet measured under the angles of 85° and 145° are scaled to the biggest line, the same is done with the calculated results (see text), the bar graphs shown correspond to an angle of 145°.

TABLE IV. Results of the multiconfiguration CI calculation (including $3d^4$, $3d^5$, and $3d^6$) for Cr at a photon energy of 720 eV.

	HF calculation		Experimental		Assignment		
Energy (eV)	Intensity	β	β	J_f	$3d^4$	$3d^5$	$3d^6$
578.77	100.0	1.23	1.04 ± 0.10	9/2		⩾98%	
579.64	52.8	0.94	1.09 ± 0.10	7/2		⩾98%	
580.12	24.1	1.23	1.09 ± 0.10	7/2		⩾98%	
580.53	42.5	1.12	1.08 ± 0.10	5/2		⩾98%	
581.13	8.7	1.21		5/2		⩾98%	
581.18	25.2	1.24	1.02 ± 0.10	3/2		⩾98%	
582.8 − 584.8	22.1	1.22	1.05 ± 0.12			⩾98%	
584.8 − 586.5	11.5	1.24	1.05 ± 0.12			⩾98%	
587.80	3.5	1.16	1.05 ± 0.10	5/2		⩾98%	
588.67 − 588.91	26.3	1.10	1.05 ± 0.10	5/2	6%	94%	
589.08	6.4	1.13		5/2	40%	55%	5%
589.11	11.6	1.19		5/2	40%	60%	
589.31	4.5	0.98		7/2		⩾98%	
589.97	10.1	1.07		7/2		⩾98%	
590.05	51.5	1.22	1.05 ± 0.10	7/2		⩾98%	

In Fig. 5 the experimental and calculated spectra of the $2p_{3/2}$ multiplet measured under an angle of 85° and 145° are shown (analogous to Fig. 3). The middle panel visualizes the nonuniformity of the calculated values for β which differs very much from the experimental results (left panel).

In contrast to Mn, investigations on the dichroism of free polarized Cr atoms [2,3] already exist. The experimentally seen dichroism (LAD as well as LMDAD) could very well be reproduced by the single configuration HF calculation only including $3d^5$. But obviously, this single configuration fails in the description of the β parameter.

Also for Cr we carried out multiconfiguration calculations including $3d^4 4s^2$, $3d^5 4s$, and $3d^6$, the results are listed in Table IV. Similar to Mn the calculated β independent cross section, the LAD, and the LMDAD for the single configuration and multiconfiguration calculations do not significantly deviate from each other (not shown). Although the expansion of the included configurations does not lead to any additional lines within the $2p_{3/2}$ multiplet, the values for β change quite remarkably, see lines at 579.6 eV and 580.5 eV in Tables III and IV. It underlines that even though these configurations are hardly admixed (see Table IV), they have a strong effect on the photoionization process. The results of this expanded calculation is visualized in the right panel of Fig. 5. It can be seen that the values of β change, however the agreement with the measurements is still not perfect.

Cr has in its ground state a $4s$ hole, whereas the $4s$ shell of Mn is filled. This results in a more complex coupling situation in the case of Cr. It is clear that there are still configurations missing in the calculation. In the case of Cr also CI with the $4p$ should be considered. Unfortunately the inclusion of these configurations leads to too many states to be handled by the computing power available today (note: the calculations presented in this paper where done on state-of-the-art parallel computing clusters and still one calculation took more than a week to be computed).

Like for Mn also for Cr it is the β parameter that poses the strongest test to the results of the ab-inito calculations. It clearly shows the influences of CI effects that cannot be revealed by measuring a different physical quantity.

V. CONCLUSION

A different experimental approach enabled us to measure the asymmetry parameter β for the $2p$ photoemission of Mn and Cr with high precision and multiplet resolved. As a result it could be shown that for Mn and Cr the values for β are uniform over the whole multiplet and also that they are similar for both elements.

The single configuration approximation calculations, which up till now have been sufficient to describe the cross section and the dichroism of free Mn and Cr atoms, fail to reproduce the values for β. Additional configurations had to be included. This means that multiplet splitting and valence shell recoupling determine the shape of the photoelectron and dichroism spectra while the dynamics of the $2p$ photoionization process is very sensitive to configuration interaction. In the case of Cr the remaining discrepancies still call for a further expansion of the calculations. Though Mn and Cr are similar in their electronic configuration, the open $4s$ shell of Cr causes a far more complex situation with regard to the number of states that have to be included for an adequate theoretical description.

APPENDIX: ANALYTICAL CALCULATION OF β WITHIN THE *jj* AND *jK* COUPLING APPROXIMATION

The dipole amplitudes in Eq. (4) can be reduced and Eqs. (2)–(4) can be considerably simplified within an approximation of pure coupling schemes. The comparison of these simplified models with intermediate coupling HF calculations allows for systematic investigation of the influence of different factors on the photoelectron angular distribution. Examples for such analyses have been presented for LSJ coupling in Ref. [23] and for jj and jK coupling in Ref. [3]. The latter study can be used here to derive the β parameter for jj and jK coupling. These coupling schemes are appropriate for core-level photoionization where the spin-orbit splitting dominates and it can be assumed that the core hole can be well described by the total angular momentum $j_0 = l_0 \pm 1/2$. For $2p$ photoionization of $3d$ metal atoms it can be assumed in a first approximation that initial and final states are described by only one electron configuration (single configuration approximation) and that all quantum numbers of the valence shells are identical in the initial atom and in the photoion (frozen valence shells). With this and in the limiting case when the second strongest interactions, the core-valence Coulomb interactions, are much stronger than the spin-orbit interactions of the valence electrons jK coupling can be applied. The core-hole angular momentum j_0 can then first be coupled to the orbital angular momentum of the valence electrons, L_0, resulting in the angular momentum K_f which then can be coupled to the total spin of the valence, shells S_0, to the total angular momentum of the final state, J_f. For the $2p$ photoionization of Mn (Cr) with $L_0 = 0$ this results in $J_f = 4$, 3, 2, and 1 ($J_f = 9/2$, 7/2, 5/2, and 3/2) for the $2p_{3/2}$ multiplet and $J_f = 3$ and 2 ($J_f = 7/2$ and 5/2) for the $2p_{1/2}$ multiplets.

Within the approximations of a single configuration, a frozen valence shell, and a pure coupling, one derives for jj coupling [3]

$$\langle \alpha_f J_f, \varepsilon l j : J || D || \alpha_0 J_0 \rangle = \hat{J}\hat{J}_f (-1)^{J+j_0+J_f+1} \begin{Bmatrix} J_0 & j_0 & J_f \\ j & J & 1 \end{Bmatrix} \times \langle \varepsilon l j || d || j_0 \rangle \tag{A1}$$

and in the case of jK coupling [3]

$$\langle \alpha_f J_f, \varepsilon l j : J || D || \alpha_0 J_0 \rangle = \hat{J}\hat{K}_f\hat{J}_0\hat{J}_f (-1)^{2J_0+L_0+S_0+J-1} \times \begin{Bmatrix} j_0 & L_0 & K_f \\ S_0 & J_f & J_0 \end{Bmatrix} \begin{Bmatrix} J_0 & j_0 & J_f \\ j & J & 1 \end{Bmatrix} \times \langle \varepsilon l j || d || j_0 \rangle . \tag{A2}$$

The reduced matrix elements $\langle \varepsilon l j || d || j_0 \rangle$ contain the one-electron wave functions of the core hole and the photoelectron only.

The dipole matrix elements can be reduced further by introducing a nonrelativistic approximation, assuming that the one-electron wave functions of the core hole ($l_0 j_0$) and of the photoelectron ($\varepsilon l j$) are independent of the values of the angular momenta j_0 and j [3]:

$$\langle \varepsilon l j || d || j_0 \rangle = \hat{j}\hat{j}_0 (-1)^{j_0+l-1/2} \begin{Bmatrix} j_0 & l_0 & \frac{1}{2} \\ l & j & 1 \end{Bmatrix} \langle \varepsilon l || d || l_0 \rangle . \tag{A3}$$

Using Eqs. (2)–(4) the angular distribution parameter β of the photoelectrons can be calculated analytically for both pure coupling schemes (jj and jK coupling):

$$\beta = \frac{(l_0+2)d_+d_+^* + (l_0-1)d_-d_-^* - 3\sqrt{l_0(l_0+1)}(d_+d_-^* + d_-d_+^*)}{(2l_0+1)[d_+d_+^* + d_-d_-^*]} \tag{A4}$$

with $d_\pm = \langle \varepsilon(l_0 \pm 1) || d || l_0 \rangle$. Now we introduce the radial integrals $R_{l_0\pm1} \geqslant 0$ and the phase shifts $\Delta_{l_0\pm1}$ which are related to $d_\pm$ by

$$d_+ = \sqrt{l_0+1} R_{l_0+1} e^{i\Delta_{l_0+1}}, \quad d_- = -\sqrt{l_0} R_{l_0-1} e^{i\Delta_{l_0-1}},$$

$$\Delta_{l_0\pm1} = \sigma_{l_0\pm1} + \delta_{l_0\pm1} - \frac{(l_0\pm1)\pi}{2}. \tag{A5}$$

$\Delta_{l_0\pm1}$ contain the phase shifts due to the long-range Coulomb potential $\sigma_{l_0\pm1}$, to the short-range atomic potential $\delta_{l_0\pm1}$ and the centrifugal potential $(l_0\pm1)\pi/2$, see Ref. [24].

Inserting Eq. (A5) in Eq. (A4) yields

$$\beta = \frac{(l_0+1)(l_0+2)R_{l_0+1}^2 + l_0(l_0-1)R_{l_0-1}^2 - 6l_0(l_0+1)R_{l_0+1}R_{l_0-1}\cos(\sigma_{l_0+1} - \sigma_{l_0-1} + \delta_{l_0+1} - \delta_{l_0-1})}{(2l_0+1)[(l_0+1)R_{l_0+1}^2 + l_0 R_{l_0-1}^2]}. \tag{A6}$$

Note that only $\sigma_{l_0\pm1}$ and $\delta_{l_0\pm1}$ are contained in Eq. A6, the additional phase shift of π (from the definition of $\Delta_{l_0\pm1}$) is compensated by a sign change of the cos term. Equation A6 is the well-known Cooper-Zare formula (see, e.g., Refs. [24,25]), which was known to be valid in central potential approximation or more generally in LS coupling for atoms having $L_0 = 0$. We have shown here that this formula is also valid, within the given approximation, for pure jj or jK coupling for arbitrary values of L_0.

[1] K. Godehusen, T. Richter, P. Zimmermann, and M. Martins, Phys. Rev. Lett. **88**, 217601 (2002).
[2] P. Wernet, J. Schulz, B. Sonntag, K. Godehusen, P. Zimmermann, M. Martins, C. Bethke, and F.U. Hillebrecht, Phys. Rev. B **62**, 14 331 (2000).
[3] P. Wernet, J. Schulz, B. Sonntag, K. Godehusen, P. Zimmermann, A.N. Grum-Grzhimailo, N.M. Kabachnik, and M. Martins, Phys. Rev. A **64**, 042707 (2001).
[4] P. Wernet, B. Sonntag, M. Martins, P. Glatzel, B. Obst, and P. Zimmermann, Phys. Rev. A **63**, 050702 (2001).
[5] A. von dem Borne, T. Dohrmann, A. Verweyen, B. Sonntag, K. Godehusen, and P. Zimmermann, Phys. Rev. Lett. **78**, 4019 (1997).
[6] P.S. Bagus, R. Broer, W. de Jong, W. Nieuwpoort, F. Parmigiani, and L. Sangaletti, Phys. Rev. Lett. **84**, 2259 (2000).
[7] M. Taguchi, T. Uozumi, and A. Kotani, J. Phys. Soc. Jpn. **66**, 247 (1997).
[8] G. van der Laan, S.S. Dhesi, and E. Dudzik, Phys. Rev. B **61**, 12 277 (2000).
[9] G. Pannaccione, G. van der Laan, H.A. Dürr, J. Vogel, and N.B. Brookes, Eur. Phys. J. B **19**, 281 (2000).
[10] G. van der Laan, J. Electron Spectrosc. Relat. Phenom. **117–118**, 89 (2001).
[11] A. von dem Borne *et al.*, Phys. Rev. A **62**, 052703 (2000).
[12] K. Godehusen, P. Zimmermann, A. Verweyen, A. von dem Borne, P. Wernet, and B. Sonntag, Phys. Rev. A **58**, R3371 (1998).
[13] K. Godehusen, H.-C. Mertins, T. Richter, P. Zimmermann, and M. Martins, Phys. Rev. A **68**, 012711 (2003).
[14] P.H. Kobrin, U. Becker, C.M. Truesdale, D.W. Lindle, H.G. Kerkhoff, and D.A. Shirley, J. Electron Spectrosc. Relat. Phenom. **34**, 129 (1984).
[15] M.O. Krause, T.A. Carlson, and A. Fahlman, Phys. Rev. A **30**, 1316 (1984).
[16] S.B. Whitfield, T. Myers, M. Bjelland, R. Wehlitz, J. Jimenez-Mier, P. Olalde-Velasco, and M.O. Krause, Phys. Rev. A **66**, 060701(R) (2002).
[17] C.N. Yang, Phys. Rev. **74**, 764 (1948).
[18] J.W. Cooper, Phys. Rev. A **42**, 6942 (1990).
[19] M.Y. Amusia, A.S. Baltenkov, L.V. Chernysheva, Z. Felfli, and A.Z. Msezane, Phys. Rev. A **63**, 052506 (2001).
[20] A.N. Grum-Grzhimailo, J. Phys. B **34**, L359 (2001).
[21] R. Cowan, *The Theory of Atomic Structure and Spectra* (University of California Press, Berkeley, 1981).
[22] S. Baier, A.N. Grum-Grzhimailo, and N.M. Kabachnik, J. Phys. B **27**, 3363 (1994).
[23] A. Verweyen, A.N. Grum-Grzhimailo, and N.M. Kabachnik, Phys. Rev. A **60**, 2076 (1999).
[24] A.F. Starace, in *Corpuscles and Radiation in Matter I*, Encyclopedia of Physics, Vol. 31 (Springer-Verlag, Berlin, 1982).
[25] C. Pan, S.L. Carter, and H.P. Kelly, Phys. Rev. A **43**, 1290 (1991).